PCCP

Accepted Manuscript

ROYAL SOCIETY OF CHEMISTRY

www.rsc.org/pccp

Cite this: DOI: 10.1039/c0xx00000x

www.rsc.org/xxxxxx

ARTICLE TYPE

Physisorption of benzene derivatives on graphene: critical roles of steric and stereoelectronic effects of the substituent

Pan-Pan Zhou,[a, b] and Rui-Qin Zhang*[c]

Received (in XXX, XXX) Xth XXXXXXXXX 20XX, Accepted Xth XXXXXXXXX 20XX

DOI: 10.1039/b000000x

A series of benzene derivatives with different substituents adsorbed on graphene was investigated using a density-functional tight-binding method with a dispersion correction. Compared to benzene, the derivative with either an electron-withdrawing or -donating substituent exhibits stronger physisorption. Moreover, the steric size of the substituent is important in determining the adsorption strength, while the direction and number of H atoms in the substituent affect the electron transfer from graphene. NBO analysis reveals that the stereoelectronic effect of conjugation between the substituent and the benzene ring strongly influences the $\pi\cdots\pi$ interaction region between the molecule and graphene. The findings can deepen the understanding of the interaction between an aromatic molecule and graphene as well as the corresponding adsorption mechanism.

Introduction

Molecular adsorption on solid surfaces has attracted great interest in the past decades due to the demand of understanding the details of the molecular behavior like affinity and its influence on the underlying surface as well as the adsorption mechanism. Graphene[1, 2] possesses unique π-electron networks which enable it to act as an excellent solid material for adsorbing metal adatoms[3-14] and inorganic[15-33] and organic[34-43] molecules, and their adsorption mechanisms were also explored based on theoretical methods. Of particular interest is the interaction between organic molecule and graphene surface via $\pi\cdots\pi$ interaction,[34-36, 39, 40, 43] because this interaction plays a significant role in chemical and biological engineering.[44, 45]

In recent years, many studies have been devoted to the origin of $\pi\cdots\pi$ interactions between organic molecules and graphene.[36, 39, 40, 43] A model case is the interaction between adenine and graphite, which shows that their $\pi\cdots\pi$ interaction is due to long-range electron correlation.[39] Similar interactions of the nucleobases adenine (A), cytosine (C), guanine (G), thymine (T), and uracil (U) with graphene have subsequently been studied, and these interactions are believed to be stabilized by a weakly attractive dispersion force due to molecular polarizability.[36] Recently, Rochefort et al. pointed out that the interaction between a substituted benzene and graphene is mainly driven by a medium-range interaction between the –COOR group and the graphene surface, but to a lesser extent by a long-range π-π interaction between the aromatic core of the adsorbate and the surface.[40] Their investigation of the adsorption of an aminotriazine on graphene suggests that this process is partly driven by the specific attractive interaction of the $-NR_2$ group with the underlying graphene surface.[43] The above results clearly indicate that the substituent is a crucial factor in determining the adsorption.

It is noteworthy that different substituents have different properties (such as electron-withdrawing or -donating), on which the adsorption strength will strongly depend. According to the Hunter-Sanders rules,[46, 47] an electron-withdrawing substituent on a benzene would result in a decrease in the π-electron density on the aromatic ring as well as the π-π repulsion between the ring and graphene, thereby leading to stronger π-π interaction. Conversely, an electron-donating substituent would lead to a weaker π-π interaction. However, the adsorption of an aniline[43] on graphene does not conform to the Hunter-Sanders rules. It is found that the aniline with an electron-donating NH_2 group has a much stronger adsorption (–14.0 kcal/mol) than benzene does (–4.5 kcal/mol). This indicates that the electron-donating group can enhance the π-π interaction, which is also observed in the aryl-aryl interaction.[48] Based on the comparison of the adsorption of a melamine and a 2,4,6-tris(dimethylamino)-1,3,5-triazine on graphene, Wuest and Rochefort suggested that the enhanced adsorption correlates with the number of H atoms in the substituent. This is because the H atom would interact with the graphene surface and accept its additional electrons.[43] However, investigations of the adsorption of a trimesic acid (TMA, with adsorption energy of –22.5 kcal/mol) and a trimethyltrimesate (TME, with adsorption energy of –23.0 kcal/mol)[40] showed that replacing the OH units of TMA with OCH_3(TME) has little effect on adsorption though the TME contains more H atoms. This result reminds us that there may be other profound and intrinsic factors influencing adsorption.

Because the adsorption strength is associated with the number of H atoms present in the adsorbate,[34, 43] the steric effect caused by a substituent, like the direction of the H atom, is also of considerable significance. One case has apparently been implicated in the adsorption of a 2-amino-1,3,5-triazine on graphene because the H atoms in the NH_2 group direct toward the

graphene surface.[43] Additionally, the larger steric size of a substituent should have a larger region of orbital overlap when interacting with graphene, so steric size is nonnegligible. On the other hand, for an aromatic compound, if its aromatic ring is conjugated with the substituent, the π-electrons would delocalize to the *p*-orbital of the substituent across an intervening sigma bond. Such a stereoelectronic effect, that is, the delocalization of π-electrons across all the adjacent aligned *p*-orbitals, generally lowers the overall energy of the molecule and increases its stability. This is known as the conjugation effect.[49] As a result, when the compound is adsorbed on graphene, the delocalization of electrons would significantly increase the π-π interacting region, which contributes to the stability of the complex. Consequently, the strength of the adsorption should be related to the extent of the conjugation between the substituent and the aromatic ring. Therefore, the present work investigates the adsorption of various benzene derivatives with different substituents (Fig. 1) on graphene to elaborate the roles of these factors.

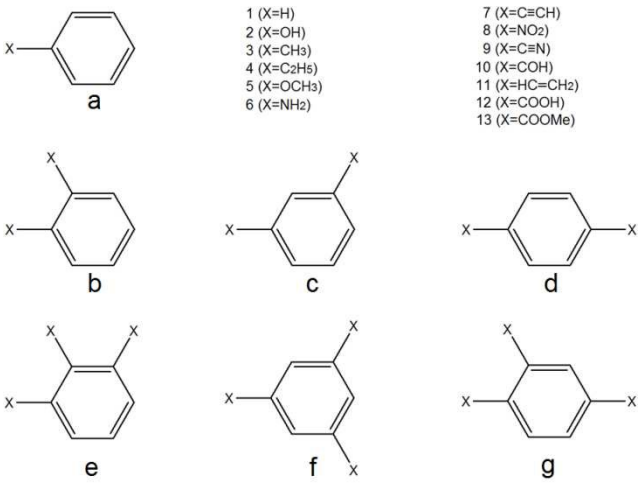

Fig. 1 Benzene and its derivatives with substituent X (**1**-**13**) at different positions (**a**-**g**).

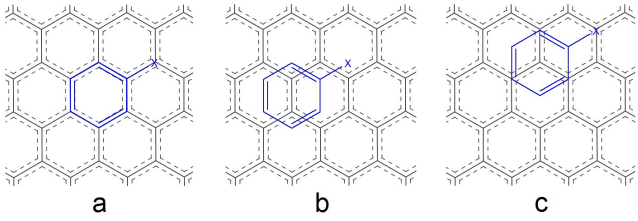

Fig. 2 An illustration of the top view of the adsorption sites of benzene or its derivative with one substituent X on a graphene sheet: (a) a hollow (H), (b) a bridge (B), (c) an on-top (O) site.

Computational methods and models

It is known that conventional density function theory (DFT) is unable to describe a complicated system correctly, especially for $\pi\cdots\pi$ interaction systems[50-52] involving dispersion force. To handle this issue, many efforts have been made to develop new methods, such as the self-consistent charge density-functional tight-binding (SCC-DFTB) method[53] with a dispersion correction,[54] and many-body dispersion (MBD) @ range-separated self-consistent screening (rsSCS) of polarizabilities (MBD@rsSCS).[55, 56] In this work, the SCC-DFTB method with a dispersion correction was employed to study the energies and geometries of the benzene derivative/graphene complexes. This method can treat very large complexes correctly and provide reliable results for weak interaction systems.[51, 53, 54, 57, 58] We used a supercell of 14.8×14.8×20.0 Å^3 consisting of a graphene sheet with 72 C atoms. On the sheet, three typical sites (a hollow site, a bridge site, and an on-top site) shown in Fig. 2 were considered as the adsorption sites. Benzene and its derivatives whose plane is parallel to the sheet were placed on these sites. For the benzene derivatives, its substituent is either electron–donating or electron-withdrawing. The single, double or triple bond connecting the substituent and benzene ring was used to estimate the effect of conjugation. The possible trial structures were designed to ensure that the contact areas between the benzene derivatives and the graphene surface are as large as possible. The trial structures designed for the derivatives with one substituent (**a1**–**13**) were fully optimized using a smart algorithm[59] with the force convergence criterion set at 0.05 kcal/mol and the charge convergence criterion set to 10^{-5} electrons. The *k*-point was set to 3×3×1 for the Brillouin zone integration. The calculations were performed using the DFTB+ program.[53, 54] A similar process was carried out to obtain the optimal configuration for the derivative with two (**b2**–**13**, **c2**–**13**, **d2**–**13**) or three (**e2**–**13**, **f2**–**13**, **g2**–**13**) substituents at different positions (*ortho*, *meta* and *para*) of benzene ring (Fig. 1).

The adsorption energy (ΔE_{ads}) of the benzene derivatives adsorbed on graphene was calculated as:

$$\Delta E_{ads} = E_{(molecule/graphene)} - E_{(molecule)} - E_{(graphene)}$$

where $E_{(molecule/graphene)}$, $E_{(molecule)}$, and $E_{(graphene)}$ denote the total energies of the relaxed molecule/graphene complex, the molecule, and graphene, respectively.

To evaluate the conjugation effect, the geometries of benzene and its derivatives (**a1**–**13**) were optimized using the M062X functional[60] with 6-31+g(d,p) basis set. The calculations were performed using the Gaussian 09 package,[61] and then natural bond orbital (NBO)[62-64] analysis was implemented at the same level to obtain the atomic orbital hybridization for the bond connecting the benzene ring with the substituent.

Results and discussion

The adsorption energies for benzene on graphene at the three sites (H, B, O) range from –13.4 to –13.5 kcal/mol (Fig. 3), agreeing with the previous theoretical (–13.5 kcal/mol[43]) and experimental (–13.6 kcal/mol[65]) values, but is quite different from the value (–4.5 kcal/mol[40, 43]) at the local density approximation (LDA) level without dispersion correction. This indicates that dispersion interaction should be taken into account because of its significant importance in stabilizing the π-π interaction. After examining the structures and energies of benzene and its derivatives on the graphene sheet, it can be found that the adsorption energies are insensitive to the adsorption sites (H, B, O), the energy difference between these sites is within 1 kcal/mol, as shown in Fig. 3. Moreover, the adsorption energies for all the derivatives are larger than that of benzene (**a1**) when one H atom in benzene is

substituted by either an electron-donating (–OH (**a2**), $–CH_3$ (**a3**), $–CH_2CH_3$ (**a4**), $–OCH_3$ (**a5**) and $–NH_2$ (**a6**)) or -withdrawing (–CCH (**a7**), $–NO_2$ (**a8**), –CN (**a9**), –COH (**a10**), $–CHCH_2$ (**a11**), –COOH (**a12**) and –COOMe (**a13**)) group.

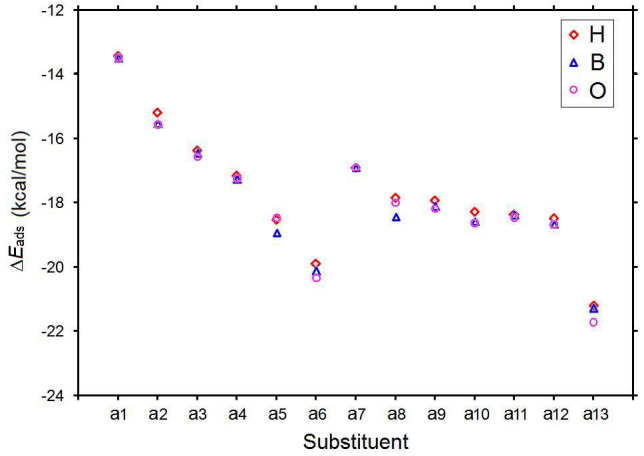

Fig. 3 The adsorption energies (ΔE_{ads}) for benzene and its derivatives (**a1**–**13**) at the adsorption sites (H, B, O) of a graphene sheet.

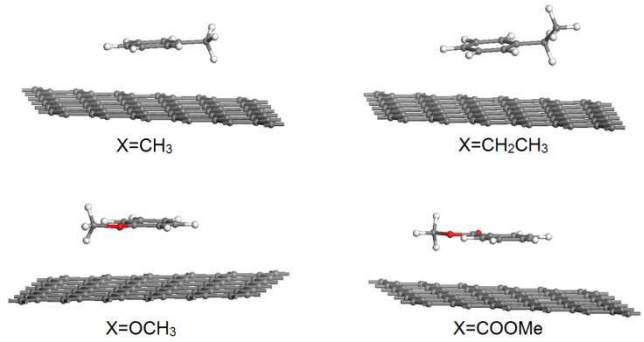

Fig. 4 The optimized geometries for the adsorption of **a3** ($X=CH_3$), **a4** ($X=CH_2CH_3$), **a5** ($X=OCH_3$) and **a13** (X=COOMe) on graphene.

In terms of the Hunter-Sanders rules,[46, 47] an electron-donating group would increase the π-electron density around the benzene ring, causing large π-π repulsion and thus obstructing the adsorption. However, *strengthened* adsorption is observed. One reason for this result is certainly the intermolecular interaction between the substituent and graphene. Because the charge transfer usually occurs from the graphene surface to the adsorbate,[66, 67] the H atom of the substituent may be directed toward the graphene surface to accept electrons coming from it. This can be described as the capacity of the molecule to accommodate additional electron density.[43] For instance, the groups $–CH_3$ (**a3**), $–CH_2CH_3$ (**a4**), $–OCH_3$ (**a5**) and $–NH_2$ (**a6**) would have the C–H or N–H bond interacting with the π ring of graphene. It may form weak C–H$\cdots\pi$ or N–H$\cdots\pi$ interactions, leading to an effective orbital overlap between the substituent and graphene and thus a strong binding. To figure out this, the minimal distances (d_m) between benzene derivatives and graphene were outlined in Table S1 (see ESI for details). As observed, the derivatives with $–CH_3$ (**a3**) and $–CH_2CH_3$ (**a4**) groups both have H atoms pointing toward the graphene surface with distances smaller than 3.0 Å (Fig. 4 and Table S1), and thus the C–H$\cdots\pi$ interactions form, strengthening the adsorption. Compared to **a3** (–16.4 kcal/mol for H site, –16.5 kcal/mol for B site, and –16.6 kcal/mol for O site), the stronger adsorption of **a4** (–17.2 kcal/mol for H site, –17.3 kcal/mol for B site, and –17.3 kcal/mol for O site) is closely related to the larger number of H atoms in the $–CH_2CH_3$ substituent as well as the interaction distance (d_m), because the two H atoms pointing toward the graphene surface with much smaller distances gain more electrons (Fig. 4 and Table S1). The larger steric size of the $–CH_2CH_3$ group also contributes. Similarly, steric effects are observed for **a2** and **a5**. Compared to the adsorption of **a2** on graphene (–15.2 kcal/mol for H site, –15.5 kcal/mol for B site, and –15.6 kcal/mol for O site), the much stronger adsorption of **a5** (–18.5 kcal/mol for H site, –18.9 kcal/mol for B site, and –18.5 kcal/mol for O site) is partly due to the larger steric size of the $–OCH_3$ group and its H atom which points toward the graphene surface. Because the possible formation of the C–H$\cdots\pi$ interaction between the $–OCH_3$ group and the graphene surface (Fig. 4) should have a strengthening effect. The stronger adsorption of the aniline (**a6**) relative to that of benzene may be connected to the H atoms of the NH_2 group because of the potential formation of an intermolecular hydrogen bond.[43] Moreover, the relationship between the Hammett sigma *meta* constant (σ_m)[68] and the interaction energies (see Fig. S1 in ESI for details) was investigated because σ_m constant can be used to measure the inductive electron-withdrawal or donation by the substituent.[69] Different from the substituent effects in benzene dimers,[69] no good correlation between ΔE_{ads} and σ_m is observed, suggesting that the substituent effects in these cases cannot be qualitatively understood according to the electron- withdrawing or donating character of the substituents. It implies that other factors should be considered in the interactions of benzene derivatives and graphene due to the huge π-electron networks of graphene.

For an electron-withdrawing group, it can be readily understood because the substituent would decrease the π-electron density around the benzene ring and thus diminish the π-π repulsion, which strengthens the adsorption. Another important contribution arises from the interaction between the substituent and graphene, as illustrated by Rochefort and Wuest.[40] The most obvious cases are the derivatives with –COOH and –COOMe groups. The adsorption energies are –18.5 kcal/mol for H site, –18.7 kcal/mol for B site, and –18.7 kcal/mol for O site for **a12**, while they are –21.2 kcal/mol for H site, –21.3 kcal/mol for B site, and –21.7 kcal/mol for O site for **a13**. In addition, it can be seen from Fig. 3 that the adsorption energies for the derivatives with the –COOH, –COOMe, and –COH groups are in the order COH (**a10**) < COOH (**a12**) < COOMe (**a13**). This can be ascribed to the different steric effects of these groups. The –COOMe group is the largest and so **a13** would have the largest orbital overlap with graphene, thus contributing to the strongest binding. Meanwhile, because the C atom of its Me group is of sp^3 hybridization, the three H atoms point in different directions. The H atom pointing toward the graphene surface with a smaller distance (Fig. 4 and Table S1) would form a weak C–H$\cdots\pi$ interaction and obtain electrons from graphene. This is another reason why it demonstrates the strongest binding. The adsorption of **a12** on graphene is a little stronger than that of **a10** (–18.2 kcal/mol for H site, –18.6 kcal/mol for B site, and –18.6 kcal/mol for O site)

because the larger steric size of the –COOH group gives a larger region of orbital overlap, relative to that of –COH group. The adsorption for **a12** (–12.2 kcal/mol) at the LDA level without dispersion correction[40] is much smaller than our results. For the derivatives with the –CCH (**a7**) and –$CHCH_2$ (**a11**) groups, the electron-withdrawing character and the different steric sizes ($CHCH_2$ > CCH) are responsible for the observed order of adsorption energies (**a11** > **a7**). However, the order in terms of electron-withdrawing abilities ($CHCH_2$ < CCH) is contrary to the ranking of adsorption energies, implying that another factor may be influencing adsorption. The extent of conjugation should be the one because of the different bonding characters (double or triple bond). For **a8** and **a9**, the adsorption is related to the strong electron-withdrawing characters of –NO_2 and –CN groups as well as the conjugation between these groups and the benzene ring. Also, the steric sizes of –NO_2 and –CN groups contribute to the bindings.

Note that the electronic structure of graphene can be tuned by adsorbing an organic molecule,[70] so the electronic properties of benzene and its derivatives adsorbing on the graphene surface could provide useful information of the substituent effect. The calculated density of states (DOS) for graphene and molecule/graphene systems were depicted in Figure S2 (see ESI for details). It is known that graphene is a zero-gap semiconductor, and its Fermi level crosses the Dirac point exactly.[71] It can be seen that the DOSs of molecule/graphene systems represent no obvious change at the Fermi level compared to graphene, so conductance change would not occur after the adsorption. In terms of frontier molecular orbital theory, the highest occupied molecular orbital (HOMO) and the lowest unoccupied molecular orbital (LUMO) are associated with the intermolecular charge transfer. For the system of molecule adsorbing on graphene, if the HOMO of molecule is higher in energy than the Fermi energy of graphene, charge transfer would occur from the molecule to graphene, while the charge transfer from graphene to the molecule would take place if the LUMO of molecule is below the Fermi energy of graphene.[23] The HOMOs and LUMOs of molecules (**a1**–**13**) were summarized in Table S2. The calculated Fermi energy for graphene is –4.64 eV, which is higher than their HOMOs and is lower than their LUMOs. It can be expected that the charge transfer between molecules (**a1**–**13**) and graphene is very weak, so the role of charge transfer interaction (e.g., N–H$\cdots\pi$ or C–H$\cdots\pi$ interaction) contributing to the adsorption is limited. It indicates that the H atom of the substituent directing toward the graphene surface could accept only small amounts of electrons.

Furthermore, the adsorption of benzene derivatives with two (**b2**–**13**, **c2**–**13**, **d2**–**13**) or three (**e2**–**13**, **f2**–**13**, **g2**–**13**) substituents at different positions of benzene ring was investigated. As shown in Fig. 5, the adsorption energies for the derivatives (**b2**–**13**, **c2**–**13**, **d2**–**13**) are somewhat sensitive to the adsorption sites (H, B, O). In some cases, the energy difference between these sites is larger than 1 kcal/mol but within 2 kcal/mol. It is noted that when the derivatives with two substituents at the *ortho*, *meta* and *para* positions adsorb on the three sites (H, B, O), they have different adsorption strength, but the energy difference is within 3 kcal/mol. It suggests that the positions of substituents affect the adsorption. Compared to the

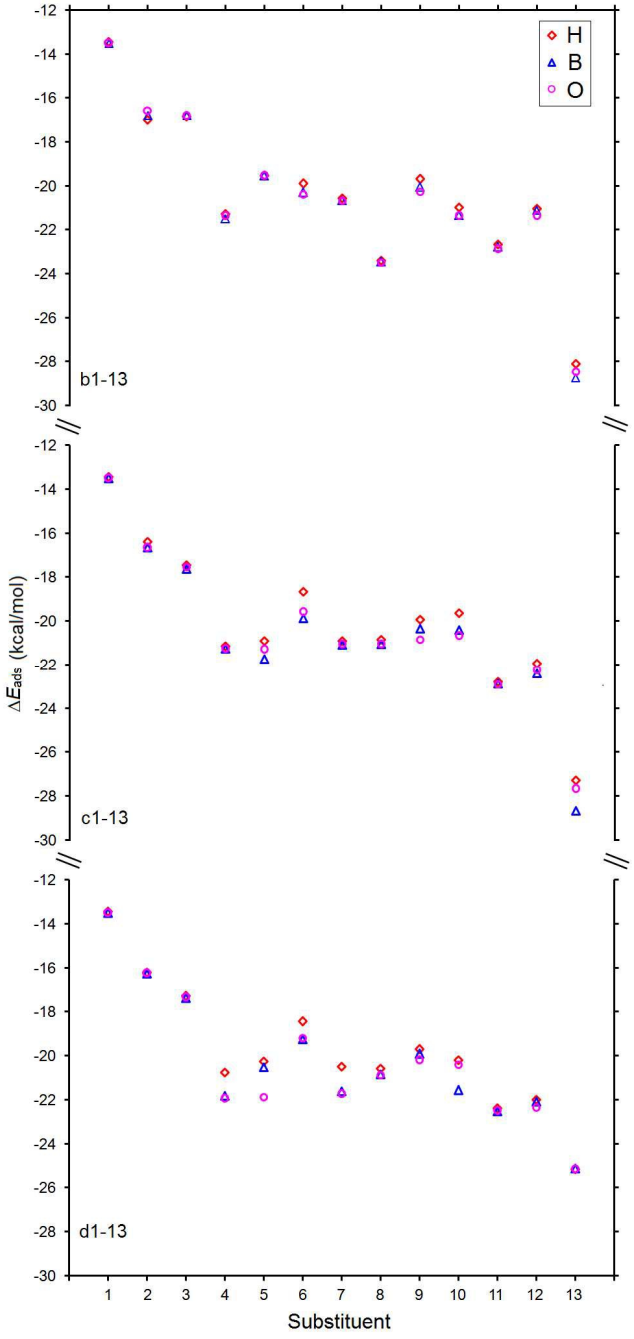

Fig. 5 The adsorption energies (ΔE_{ads}) for benzene and its derivatives (**b1**–**13**, **c1**–**13**, **d1**–**13**, **b1=c1=d1=benzene**) at the adsorption sites (H, B, O) of a graphene sheet.

derivatives with one substituent (**a1**–**13**), the derivatives (**b2**–**13**, **c2**–**13**, **d2**–**13**) have stronger adsorption. When an electron-donating group is added to the *ortho*, *meta* and *para* positions of **a2**–**6**, the corresponding derivatives (**b**, **c**, **d**) with –OH, –CH_3 and –NH_2 substituents have small increments (ca. 1 kcal/mol) of adsorption energies, but the corresponding derivatives with –CH_2CH_3 and –OCH_3 substituents have increments ranging from 1 to 5 kcal/mol. When an electron-withdrawing group is added, large increments (2–8 kcal/mol) are observed for the corresponding **b7**–**13**, **c7**–**13**, **d7**–**13**. Note that the adsorption for **c12** (–19.5 kcal/mol) at the LDA level without dispersion

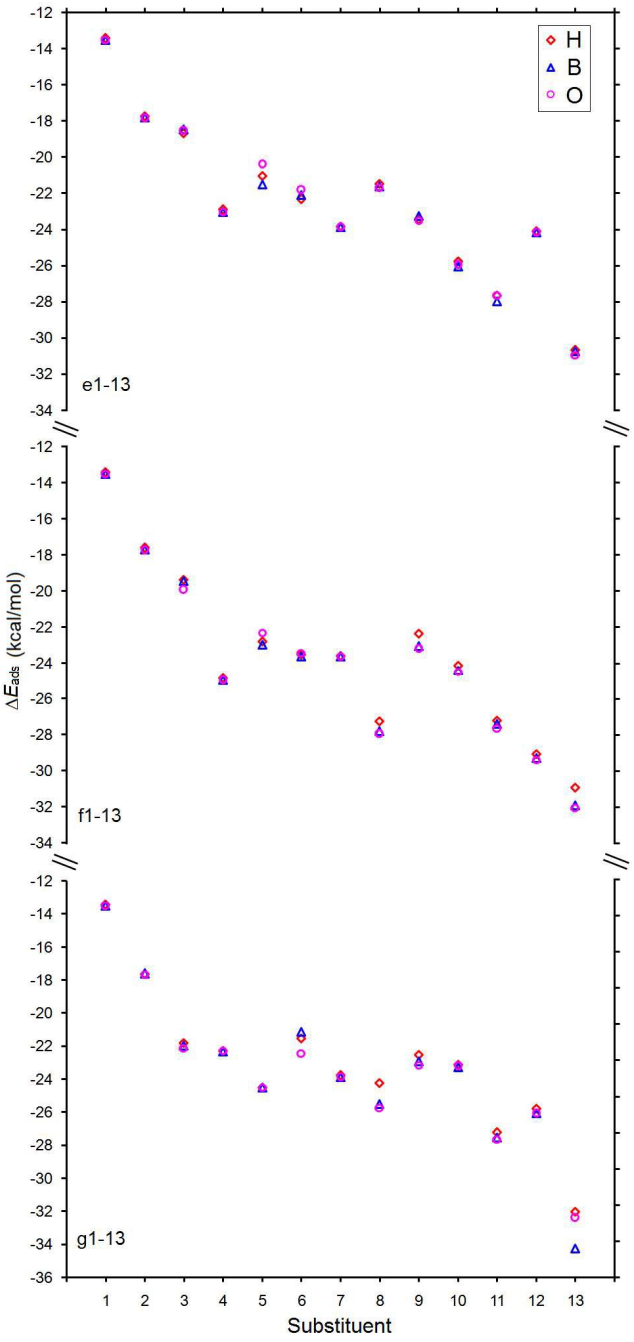

Fig. 6 The adsorption energies (ΔE_{ads}) for benzene and its derivatives (**e1**–**13**, **f1**–**13**, **g1**–**13**, **e1=f1=g1=benzene**) at the adsorption sites (H, B, O) of a graphene sheet.

correction[40] is also much smaller than our results (–21.9 kcal/mol for H site, –22.4 kcal/mol for B site, and –22.3 kcal/mol for O site). Fig. 6 shows the adsorption energies for the derivatives (**e2**–**13**, **f2**–**13**, **g2**–**13**) with three substituents. They have stronger adsorption than those of **a1**–**13**, **b2**–**13**, **c2**–**13**, and **d2**–**13**. The adsorption energies are sensitive to the sites (H, B, O) for some cases like **e5**, **f6**, **f8**, **f13**, **g13**, and the energy difference is within 2 kcal/mol between different sites. Also, the positions of the substituents influence the adsorption. For instance, the three –NO_2 groups of **e8** are very close to each other, resulting in strong steric repulsion. Thereby, the three groups are not coplanar with the benzene ring, and the weaker adsorption is observed relative to those of **f8** and **g8**. The similar phenomena is also observed for **e12**. The adsorption of TMA (**f12**, with adsorption energies of –25.8 kcal/mol for H site, –26.1 kcal/mol for B site, and –26.1 kcal/mol for O site) and TME (**f13**, with adsorption energies of –32.0 kcal/mol for H site, –34.3 kcal/mol for B site, and –32.4 kcal/mol for O site) on graphene further confirms that the –OH as well as the –OCH_3 group also interacts with graphene, and the –OCH_3 group makes a relatively larger contribution. This is inconsistent with previous work which concludes that replacing the –OH unit with an –OCH_3 has little effect on adsorption.[40] The reason for this is that the calculation carried out at the LDA level did not consider the dispersion correction,[40] and thus did not include the possible contribution arising from the interaction between the –OH or –OCH_3 unit and the graphene surface. Our results show that besides the C=O unit, the –OH and –OCH_3 units also participate in the interaction with the graphene surface through weak dispersion interactions.

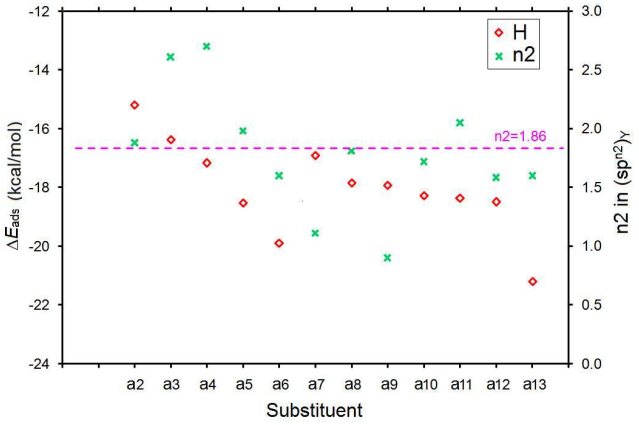

Fig. 7 The relationship between adsorption energy (ΔE_{ads} at the H site) for the derivative with one substituent and n2 in the $(sp^{n2})_Y$ atomic hybrid state (the dashed pink line indicates the hybrid state of C atom $[(sp^{1.86})_C]$ of benzene in which n2=1.86). Only ΔE_{ads} at the H site is used because of the insensitivity of ΔE_{ads} to the adsorption sites (H, B, O).

In addition, the conjugation effect was also analyzed and the results are shown in Table 1. The $(sp^{n2})_Y$ hybrid state is indicative of the conjugation character of the Y atom connecting to the C atom of benzene. The closer the hybrid state of Y atom to that of the C atom $[(sp^{1.86})_C]$ of benzene, the stronger the extent of conjugation. Consequently, the π-electrons would be easier to delocalize across all adjacent and aligned *p*-orbitals. This leads not only to a decrease of the π-electron density on the benzene ring but of the even larger π-interacting region of the whole molecule, because the conjugating atom or group is involved in the π-π interaction. Therefore, the extent of conjugation is also an important factor in determining adsorption. As shown in Table 1, **a2** has $(sp^{1.88})_O$ hybrid state for its O atom, which is close to that of benzene (Fig. 7), indicating the good conjugation between O and the aromatic ring. This would decrease the π-electron density of the aromatic ring and thus counterbalence its electron-donating effect. It explains the stronger adsorption relative to that of benzene. The derivatives **a3** and **a4** have $(sp^{2.61})_C$ and $(sp^{2.70})_C$ hybrid states for their C atoms, respectively. These significantly deviate from that of benzene (Table 1), and their n2 values are far away from the pink line in Fig. 7. Compared to **a2**, a stronger

Cite this: DOI: 10.1039/c0xx00000x

www.rsc.org/xxxxxx

ARTICLE TYPE

Table 1 The atomic orbital hybridization for the bond connecting the benzene ring with the substituent X.

Molecule	σ_{CY} [a]				σ_{CY}^* [a]			
	C_C	C_Y	$(sp^{n1})_C$	$(sp^{n2})_Y$	C_C	C_Y	$(sp^{n1})_C$	$(sp^{n2})_Y$
a1 (Benzene)	0.792	0.611	$(sp^{2.32})_C$	$(s)_H$	0.611	0.792	$(sp^{2.32})_C$	$(s)_H$
a2	0.578	0.816	$(sp^{2.99})_C$	$(sp^{1.88})_O$	0.816	0.578	$(sp^{2.99})_C$	$(sp^{1.88})_O$
a3	0.715	0.699	$(sp^{2.15})_C$	$(sp^{2.61})_C$	0.699	0.715	$(sp^{2.15})_C$	$(sp^{2.61})_C$
a4	0.712	0.702	$(sp^{2.14})_C$	$(sp^{2.70})_C$	0.702	0.712	$(sp^{2.14})_C$	$(sp^{2.70})_C$
a5	0.570	0.822	$(sp^{3.03})_C$	$(sp^{1.98})_O$	0.822	0.570	$(sp^{3.03})_C$	$(sp^{1.98})_O$
a6	0.635	0.773	$(sp^{2.48})_C$	$(sp^{1.60})_N$	0.773	0.635	$(sp^{2.48})_C$	$(sp^{1.60})_N$
a7	0.714	0.701	$(sp^{2.25})_C$	$(sp^{1.11})_C$	0.701	0.714	$(sp^{2.25})_C$	$(sp^{1.11})_C$
a8	0.609	0.793	$(sp^{3.25})_C$	$(sp^{1.81})_N$	0.793	0.609	$(sp^{3.25})_C$	$(sp^{1.81})_N$
a9	0.714	0.700	$(sp^{2.46})_C$	$(sp^{0.90})_C$	0.700	0.714	$(sp^{2.46})_C$	$(sp^{0.90})_C$
a10	0.730	0.684	$(sp^{2.29})_C$	$(sp^{1.72})_C$	0.684	0.730	$(sp^{2.29})_C$	$(sp^{1.72})_C$
a11	0.718	0.696	$(sp^{2.10})_C$	$(sp^{2.05})_C$	0.696	0.718	$(sp^{2.10})_C$	$(sp^{2.05})_C$
a12	0.721	0.693	$(sp^{2.41})_C$	$(sp^{1.59})_C$	0.693	0.721	$(sp^{2.41})_C$	$(sp^{1.59})_C$
a13	0.720	0.694	$(sp^{2.40})_C$	$(sp^{1.60})_C$	0.694	0.720	$(sp^{2.40})_C$	$(sp^{1.60})_C$

[a] The general form for the C–Y bond can be represented as: $\sigma_{CY} = C_C(sp^{n1})_C + C_Y(sp^{n2})_Y$ for the bonding orbital, and $\sigma_{CY}^* = C_C(sp^{n1})_C - C_Y(sp^{n2})_Y$ for the antibonding orbital, where C_C and C_Y are the polarization coefficients for the carbon atom of benzene ring and Y atom of the substituent, respectively. The natural atomic hybrids $(sp^{n1})_C$ and $(sp^{n2})_Y$ are the components for the natural bond orbital of C–Y bond.

adsorption but less conjugation was observed for **a3** as well as **a4**. This suggests that the lesser conjugation has little effect on adsorption, which is dominated by other factors (such as the steric size of the substituent, its direction, and the number of H atoms). The Y atom hybrid states of **a5** and **a6** are $(sp^{1.98})_O$ and $(sp^{1.60})_N$, respectively. They approach that of benzene (Table 1 and Fig. 7), suggesting the formations of well conjugated systems. The expanded π-interacting regions of **a5** and **a6** due to π-electron delocalization would certainly produce stronger π-π interactions relative to benzene, even though both the $-OCH_3$ and $-NH_2$ groups are electron-donating. In comparison with **a2**, the lesser conjugation of the O atom for **a5** is observed, but the adsorption of **a5** on graphene is even stronger. This can be ascribed to the larger number of H atoms and the larger steric size of the $-OCH_3$ group relative to that of the OH group. For **a7** and **a9**, the triple bonds of the ethynyl and cyano-group are not conjugated with benzene rings, as can be seen from their hybrid states of $(sp^{1.11})_C$ and $(sp^{0.90})_C$, indicating the small effect of hybridization on their adsorption. In contrast with **a6**, a similar hybrid state of the N atom $[(sp^{1.81})_N]$ for **a8** is found, approaching to that of benzene. But the stronger adsorption for **a8** is observed. Obviously, besides the conjugation, other factors (such as the very strong electron-withdrawing character and larger steric size of the $-NO_2$ group, and its special structure with electron delocalization which further extends the π-interacting region) are also responsible for the adsorption. With respect to **a10**, **a12** and **a13**, the hybrid states of the C atoms in the –COH, –COOH and –COOMe groups are close to that of benzene (Table 1 and Fig. 7), indicating that electron delocalization occurs in these compounds but to a different extent. Consequently, such conjugation certainly contributes to the adsorption. While the order of adsorption (**a13** > **a12** > **a10**) confirms that the steric size and the number of H atoms as well as their directions are also of great importance. The Y atom of **a11** (Y=C) has a $(sp^{2.05})_C$ hybrid state close to that of benzene, indicating that the C=C double bond of the vinyl is well conjugated with the aromatic ring. Accordingly, the stronger adsorption of **a11** relative to those of **a3**, **a4**, and **a7** is found, as can be seen from Fig. 7, which shows that the conjugation plays a dominant role. For these compounds (**a2**–**a13**), the correlation between the adsorption and hybridization (Fig. 7) shows that a benzene derivative having good conjugation undoubtedly contributes to a strong adsorption, but the aforementioned factors should also be taken into account. For compounds with less conjugation, these other factors should dominate.

To further assess the importance of the factors (that is, the steric size of the substituent, the direction of the H atom relative to graphene, the number of H atoms in the substituent directing to the graphene surface, and the conjugation effect), we assume that graphene grows from a small aromatic molecule to a big one (polyaromatic ring), using the representative examples $C_{10}H_8$, $C_{14}H_{10}$, $C_{24}H_{12}$ and $C_{42}H_{14}$. Their interactions with benzene and the derivatives (**a3**, **a4**, **a7**, **a11**) were investigated using the DFTB+ method. The adsorption energy was calculated by using the equation (ΔE_{ads}) adopted in the previous calculations for the molecule/graphene complex.

The interactions of the derivative with the aromatic molecules become stronger as the number of C atoms increases, as shown in Fig. 8. This suggests that to get an accurate interaction energy, the graphene adopted in the adsorption model should be large enough to ensure that the interacting region accommodates the whole derivative because of the steric size. The order of adsorption for **a1** (benzene), **a3**, and **a4** (that is, **a1** < **a3** < **a4**) is closely related to the direction of the H atoms and the number of them directed toward the surface of the aromatic ring. Because **a1** and **a3** have one and two H atoms directing toward the surface of the aromatic molecule, they may form weak C–H$\cdots\pi$ interactions. The electron transfer through the C–H$\cdots\pi$ interaction would strengthen the adsorption. The interactions between **a7** and the aromatic molecules are weaker than those of

a4, suggesting the important roles of the number and direction of H atoms, as observed in **a4**. The $-CHCH_2$ group in **a11** is almost coplanar with the benzene ring, and thus there is no H atom directing toward the surface of the aromatic molecule, but the adsorption energy is stronger than that of **a4**. Obviously, the conjugation between the $-CHCH_2$ group and the benzene ring expands the π-interacting region of **a11** and leads to a strong π-π interaction during adsorption. In contrast with **a7**, the stronger adsorption of **a11** is ascribed to its better conjugation effect. Surprisingly, when the number of C atoms rises from 10 to 14, the interactions between **a7** and the aromatic molecules are weaker than those of **a3**, but are stronger than them when the number of C atoms increases from 16 to 42. Evidently, when the smaller adsorption model ($C_{10}H_8$, $C_{14}H_{10}$) is adopted, the contribution from the H atom in the $-CH_3$ group of **a3** (which is directed toward the surfaces of the aromatic rings to obtain additional electrons and thus strengthens adsorption) is larger than that arising from the electron-withdrawing character of the –CCH group (which diminishes the π-π repulsion and thus strengthens adsorption). In contrast, because the adsorption model ($C_{16}H_{10}$, $C_{24}H_{12}$ and $C_{42}H_{14}$) adopted is large enough to interact with **a7**, the larger steric size of its –CCH group has a larger orbital overlap with the them. This effect, combined with the electron-withdrawing character of the –CCH group, surpasses the effect of the H atom in the $-CH_3$ group of **a3**. Thereby, the adsorption energy for **a7** becomes stronger than that of **a3** when $C_{16}H_{10}$, $C_{24}H_{12}$ or $C_{42}H_{14}$ is adopted. The stronger adsorption for **a7** relative to benzene indicates that the electron-withdrawing character of the –CCH group plays a dominant role, which is consistent with the Hunter-Sanders rules.[46, 47]

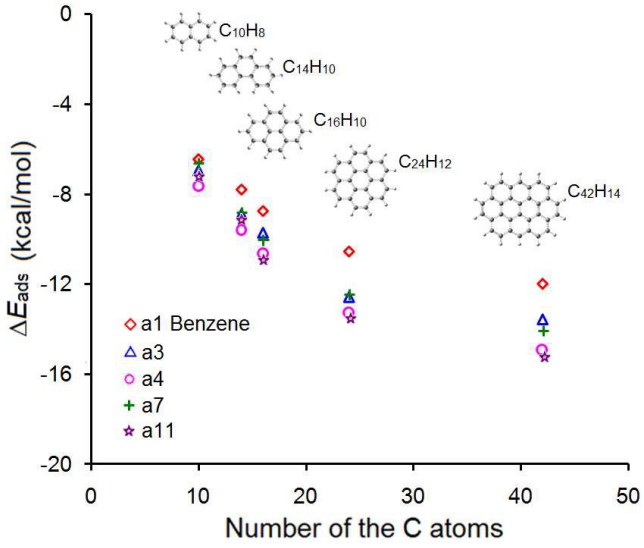

Fig. 8 The adsorption energies (ΔE_{ads}) of $C_{10}H_8$, $C_{14}H_{10}$, $C_{16}H_{10}$, $C_{24}H_{12}$ and $C_{42}H_{14}$ with benzene (**a1**) and the derivatives (**a3**, **a4**, **a7**, **a11**) versus the number of C atoms in the polyaromatic molecules.

Conclusions

Compared to the adsorption of benzene on graphene, the derivatives exhibit stronger adsorption energies regardless of the electronic property of the substituent, whether electron-withdrawing or -donating. A substituent with a larger steric size has a larger region of orbital overlap, and one with H atoms directed toward the graphene surface could gain additional electrons from it. If either of these factors is present, the adsorption energy will be enhanced. Meanwhile, the number of H atoms in the substituent may be related to the capacity of the molecule to accommodate additional electrons, which is also a factor influencing adsorption. In addition, the conjugation between the substituent and the aromatic ring is very important because it not only reduces the π-electron density around the ring because of the electron delocalization, but also forms a larger π-interacting region in the π-π interaction. The molecular properties like the electron-withdrawing or -donating ability are also important, while we note that these properties can be assessed by employing the Information Conservation Principle[72, 73] to determine the molecular electrophilicity and nucleophilicity. Therefore, a comprehensive understanding of the origin of adsorption should take all these factors into account.

Acknowledgments

The work described in this paper is supported by a grant from the Research Grants Council of Hong Kong SAR [project No. CityU 103812]. PZ thanks the financial support by the National Natural Science Foundation of China (Grant No. 21403097) and the Fundamental Research Funds for the Central Universities (lzujbky-2014-182).

Notes and references

[a] *Beijing Computational Science Research Center, Beijing, 100084, P. R. China*
[b] *Department of Chemistry, Lanzhou University, Lanzhou 730000, P. R. China*
[c] *Department of Physics and Materials Science, City University of Hong Kong, Hong Kong SAR, P. R. China; Fax: +852 3442 0538; Tel: +852 3442 7849; E-mail: aprqz@cityu.edu.hk*

† Electronic Supplementary Information (ESI) available: the minimal distances (d_m) between benzene derivatives and graphene, the HOMO and LUMO orbital energies for molecules (**a1-13**), the relationship between the Hammett sigma meta constant and the interaction energies, the total electronic DOSs for graphene and molecule/graphene systems with three different adsorption (H, B, O) sites. See DOI: 10.1039/b000000x/.

1. A. K. Geim and K. S. Novoselov, *Nat. Mater.*, 2007, **6**, 183.
2. K. S. Novoselov, A. K. Geim, S. V. Morozov, D. Jiang, Y. Zhang, S. V. Dubonos, I. V. Grigorieva and A. A. Firsov, *Science*, 2004, **306**, 666.
3. M. Amft, S. Lebegue, O. Eriksson and N. V. Skorodumova, *J. Phys.: Condens. Matter*, 2011, **23**, 395001.
4. C. Cao, M. Wu, J. Jiang and H.-P. Cheng, *Phys. Rev. B*, 2010, **81**, 205424.
5. K. T. Chan, J. B. Neaton and M. L. Cohen, *Phys. Rev. B*, 2008, **77**, 235430.
6. J. Granatier, P. Lazar, M. Otyepka and P. Hobza, *J. Chem. Theory Comput.*, 2011, **7**, 3743.
7. P. A. Khomyakov, G. Giovannetti, P. C. Rusu, G. Brocks, J. van den Brink and P. J. Kelly, *Phys. Rev. B*, 2009, **79**, 195425.
8. X. Liu, C. Z. Wang, M. Hupalo, Y. X. Yao, M. C. Tringides, W. C. Lu and K. M. Ho, *Phys. Rev. B*, 2010, **82**, 245408.
9. A. Lugo-Solis and I. Vasiliev, *Phys. Rev. B*, 2007, **76**, 235431.
10. Y. Mao, J. Yuan and J. Zhong, *J. Phys.: Condens. Matter*, 2008, **20**, 115209.

11. P. V. C. Medeiros, F. de BritoMota, A. J. S. Mascarenhas and C. M. C. de Castilho, *Nanotechnology*, 2010, **21**, 115701.
12. Y. Sanchez-Paisal, D. Sanchez-Portal and A. Ayuela, *Phys. Rev. B*, 2009, **80**, 045428.
13. Y.-H. Zhang, K.-G. Zhou, K.-F. Xie, H.-L. Zhang, Y. Peng and C.-W. Wang, *Phys. Chem. Chem. Phys.*, 2012, **14**, 11626.
14. H. Zhou, F. Yu, D. Tang, M. Chen, H. Yang, G. Wang, Y. Guo and L. Sun, *Nanoscale*, 2013, **5**, 124.
15. D. W. Boukhvalov, M. I. Katsnelson and A. I. Lichtenstein, *Phys. Rev. B*, 2008, **77**, 035427.
16. F. Costanzo, P. L. Silvestrelli and F. Ancilotto, *J. Chem. Theory Comput.*, 2012, **8**, 1288.
17. Y. Ferro, D. Teillet-Billy, N. Rougeau, V. Sidis, S. Morisset and A. Allouche, *Phys. Rev. B*, 2008, **78**, 085417.
18. P. Giannozzi, R. Car and G. Scoles, *J. Chem. Phys.*, 2003, **118**, 1003.
19. I. Hamada, *Phys. Rev. B*, 2012, **86**, 195436.
20. D. Henwood and J. D. Carey, *Phys. Rev. B*, 2007, **75**, 245413.
21. V. V. Ivanovskaya, A. Zobelli, D. Teillet-Billy, N. Rougeau, V. Sidis and P. R. Briddon, *Eur. Phys. J. B*, 2010, **76**, 481.
22. K. C. Kemp, H. Seema, M. Saleh, N. H. Le, K. Mahesh, V. Chandra and K. S. Kim, *Nanoscale*, 2013, **5**, 3149.
23. O. Leenaerts, B. Partoens and F. M. Peeters, *Phys. Rev. B*, 2008, **77**, 125416.
24. O. Leenaerts, B. Partoens and F. M. Peeters, *Appl. Phys. Lett.*, 2008, **92**, 243125.
25. O. Leenaerts, B. Partoens and F. M. Peeters, *Microelectr. J.*, 2009, **40**, 860.
26. O. Leenaerts, B. Partoens and F. M. Peeters, *Phys. Rev. B*, 2009, **79**, 235440.
27. J. Ma, A. Michaelides, D. Alfe, L. Schimka, G. Kresse and E. Wang, *Phys. Rev. B*, 2011, **84**, 033402.
28. H. E. Romero, P. Joshi, A. K. Gupta, H. R. Gutierrez, M. W. Cole, S. A. Tadigadapa and P. C. Eklund, *Nanotechnology*, 2009, **20**, 245501.
29. A. N. Rudenko, F. J. Keil, M. I. Katsnelson and A. I. Lichtenstein, *Phys. Rev. B*, 2010, **82**, 035427.
30. L. Sheng, Y. Ono and T. Taketsugu, *J. Phys. Chem. C*, 2010, **114**, 3544.
31. M. H. F. Sluiter and Y. Kawazoe, *Phys. Rev. B*, 2003, **68**, 085410.
32. R. X. Song, S. Wangmo, M. S. Xin, Y. Meng, P. Huai, Z. G. Wang and R. Q. Zhang, *Nanoscale*, 2013, **5**, 6767.
33. T. O. Wehling, A. I. Lichtenstein and M. I. Katsnelson, *Appl. Phys. Lett.*, 2008, **93**, 202110.
34. J. Björk, F. Hanke, C.-A. Palma, P. Samori, M. Cecchini and M. Persson, *J. Phys. Chem. Lett.*, 2010, **1**, 3407.
35. S. D. Chakarova-Käck, E. Schröder, B. I. Lundqvist and D. C. Langreth, *Phys. Rev. Lett.*, 2006, **96**, 146107.
36. S. Gowtham, R. H. Scheicher, R. Ahuja, R. Pandey and S. P. Karna, *Phys. Rev. B*, 2007, **76**, 033401.
37. P. Lazar, F. Karlický, P. Jurečka, M. Kocman, E. Otyepková, K. Šafářová and M. Otyepka, *J. Am. Chem. Soc.*, 2013, **135**, 6372-6377.
38. Y. H. Lu, W. Chen, Y. P. Feng and P. M. He, *J. Phys. Chem. B*, 2009, **113**, 2.
39. F. Ortmann, W. G. Schmidt and F. Bechstedt, *Phys. Rev. Lett.*, 2005, **95**, 186101.
40. A. Rochefort and J. D. Wuest, *Langmuir*, 2009, **25**, 210.
41. A. Schlierf, H. Yang, E. Gebremedhn, E. Treossi, L. Ortolani, L. Chen, A. Minoia, V. Morandi, P. Samori, C. Casiraghi, D. Beljonne and V. Palermo, *Nanoscale*, 2013, **5**, 4205.
42. C. Thierfelder, M. Witte, S. Blankenburg, E. Rauls and W. G. Schmidt, *Surf. Sci.*, 2011, **605**, 746.
43. J. D. Wuest and A. Rochefort, *Chem. Commun.*, 2010, **46**, 2923.
44. F. J. M. Hoeben, P. Jonkheijm, E. W. Meijer and A. Schenning, *Chem. Rev.*, 2005, **105**, 1491.
45. E. A. Meyer, R. K. Castellano and F. Diederich, *Angew. Chem. Int. Ed.*, 2003, **42**, 1210.
46. C. A. Hunter, *Angew. Chem. Int. Ed.*, 1993, **32**, 1584.
47. C. A. Hunter and J. K. M. Sanders, *J. Am. Chem. Soc.*, 1990, **112**, 5525.
48. S. E. Wheeler, A. J. Mcneil, P. Muller, T. M. Swager and K. N. Houk, *J. Am. Chem. Soc.*, 2010, **132**, 3304.
49. M. Jerry, *Advanced Organic Chemistry reactions, mechanisms and structure*, 3rd ed. edn., John Wiley & Sons, inc, New York, 1985.
50. W. M. Sun, Y. X. Bu and Y. X. Wang, *J. Phys. Chem. B*, 2008, **112**, 15442.
51. C. H. Wang, S. Li, R. Q. Zhang and Z. J. Lin, *Nanoscale*, 2012, **4**, 1146.
52. Y. X. Wang, *J. Phys. Chem. C*, 2008, **112**, 14297.
53. M. Elstner, D. Porezag, G. Jungnickel, J. Elsner, M. Haugk, T. Frauenheim, S. Suhai and G. Seifert, *Phys. Rev. B*, 1998, **58**, 7260.
54. M. Elstner, P. Hobza, T. Frauenheim, S. Suhai and E. Kaxiras, *J. Chem. Phys.*, 2001, **114**, 5149.
55. A. Ambrosetti, A. M. Reilly, J. DiStasio, R. A. and A. Tkatchenko, *J. Chem. Phys.*, 2014, **140**, 18A508.
56. A. Tkatchenko, J. DiStasio, R. A., R. Car and M. Scheffler, *Phys. Rev. Lett.*, 2012, **108**, 236402.
57. M. Elstner, T. Frauenheim and S. Suhai, *J. Mole. Struct (THEOCHEM)*, 2003, **632**, 29.
58. C. S. Lin, R. Q. Zhang, T. A. Niehaus and T. Frauenheim, *J. Phys. Chem. C*, 2007, **111**, 4069.
59. M. S. Amer, J. A. Elliott, J. F. Maguire and A. H. Windle, *Chem. Phys. Lett.*, 2005, **411**, 395-398.
60. Y. Zhao and D. G. Truhlar, *Acc. Chem. Res.*, 2008, **41**, 157.
61. M. J. Frisch, G. W. Trucks, H. B. Schlegel, G. E. Scuseria, M. A. Robb, J. R. Cheeseman, G. Scalmani, V. Barone, B. Mennucci, G. A. Petersson, H. Nakatsuji, M. Caricato, X. Li, H. P. Hratchian, A. F. Izmaylov, J. Bloino, G. Zheng, J. L. Sonnenberg, M. Hada, M. Ehara, K. Toyota, R. Fukuda, J. Hasegawa, M. Ishida, T. Nakajima, Y. Honda, O. Kitao, H. Nakai, T. Vreven, J. A. Montgomery, Jr., J. E. Peralta, F. Ogliaro, M. Bearpark, J. J. Heyd, E. Brothers, K. Kudin, N., V. N. Staroverov, R. Kobayashi, J. Normand, K. Raghavachari, A. Rendell, J. C. Burant, S. S. Iyengar, J. Tomasi, M. Cossi, N. Rega, N. J. Millam, M. Klene, J. E. Knox, J. B. Cross, V. Bakken, C. Adamo, J. Jaramillo, R. Gomperts, R. E. Stratmann, O. Yazyev, A. J. Austin, R. Cammi, C. Pomelli, J. W. Ochterski, R. L. Martin, K. Morokuma, V. G. Zakrzewski, G. A. Voth, P. Salvador, J. J. Dannenberg, S. Dapprich, A. D. Daniels, O. Farkas, J. B. Foresman, J. V. Ortiz, J. Cioslowski and D. J. Fox, Gaussian, Inc., Wallingford CT, Gaussian 09, Revision, A. 02, 2009.
62. J. P. Foster and F. Weinhold, *J. Am. Chem. Soc.*, 1980, **102**, 7211.
63. A. E. Reed, L. A. Curtiss and F. Weinhold, *Chem. Rev.*, 1988, **88**, 899.
64. A. E. Reed, R. B. Weinstock and F. Weinhold, *J. Chem. Phys.*, 1985, **83**, 735.
65. R. Zacharia, H. Ulbricht and T. Hertel, *Phys. Rev. B*, 2004, **69**, 155406.
66. F. Schedin, A. K. Geim, S. V. Morozov, E. W. Hill, P. Blake, M. I. Katsnelson and K. S. Novoselov, *Nat. Mater.*, 2007, **6**, 652.
67. T. O. Wehling, K. S. Novoselov, S. V. Morozov, E. E. Vdovin, M. I. Katsnelson, A. K. Geim and A. I. Lichtenstein, *Nano Lett.*, 2008, **8**, 173.
68. C. Hansch, A. Leo and R. W. Taft, *Chem. Rev.* , 1991, **91**, 165.
69. S. E. Wheeler and K. N. Houk, *J. Am. Chem. Soc.*, 2008, **130**, 10854.
70. Y. H. Lu, W. Chen, Y. P. Feng and P. M. He, *J. Phys. Chem. B*, 2009, **113**, 2.
71. Y.-H. Zhang, K.-G. Zhou, K.-F. Xie, J. Zeng, H.-L. Zhang and Y. Peng, *Nanotechnology*, 2010, **21**, 065201.
72. X.-Y. Zhou, C.-Y. Rong, T. Lu and S.-B. Liu, *Acta Phys. -Chim. Sin.*, 2014, **30**, 2055.
73. S. Liu, C. Rong and T. Lu, *J. Phys. Chem. A*, 2014, **118**, 3698.

Table of Contents

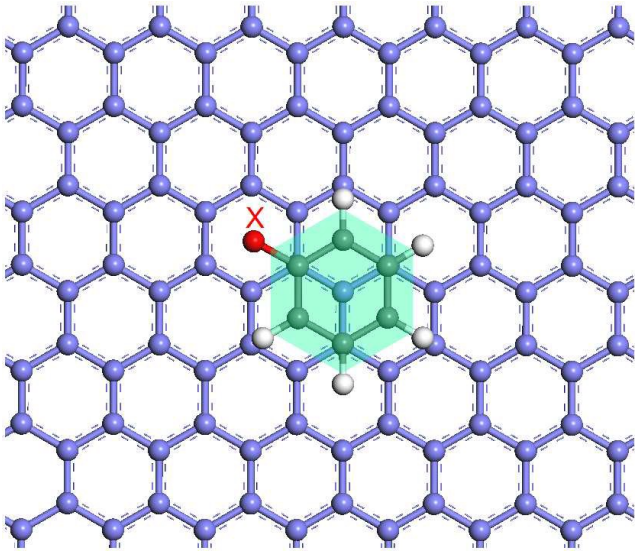

The adsorption of benzene derivative on the graphene surface is strongly dependent upon the substituent because of the critical roles of its steric and stereoelectronic effects.